Determination of a source in the heat equation from integral observations

Dinh Nho Hào[1,2], Phan Xuan Thanh[3], D. Lesnic[2], and M. Ivanchov[4]
[1] *Hanoi Institute of Mathematics, 18 Hoang Quoc Viet Road, Hanoi, Vietnam*
e-mail: hao@math.ac.vn
[2] *Department of Applied Mathematics, University of Leeds, Leeds LS2 9JT, UK*
e-mail: amt5ld@maths.leeds.ac.uk
[3] *School of Applied Mathematics and Informatics,*
Hanoi University of Science and Technology, 1 Dai Co Viet Road, Hanoi, Vietnam
e-mail: thanh.phanxuan@hust.vn
[4] *Faculty of Mechanics and Mathematics, Ivan Franko National University of Lviv,*
1 Universytetska Str., Lviv, 79000 Ukraine
e-mail: ivanchov@franko.lviv.ua

November 5, 2013

Abstract

A novel inverse problem which consists of the simultaneous determination of a source together with the temperature in the heat equation from integral observations is investigated. These integral observations are weighted averages of the temperature over the space domain and over the time interval. The heat source is sought in the form of a sum of two space- and time-dependent unknown components in order to ensure uniqueness of solution. The local existence and uniqueness of the solution in classical Hölder spaces are proved. The inverse problem is linear, but it is ill-posed because small errors in the input integral observations cause large errors in the output source. For a stable reconstruction a variational least-squares method with or without penalization is employed. The gradient of the functional which is minimized is calculated explicitly and the conjugate gradient method is applied. Numerical results obtained for several benchmark test examples show accurate and stable numerical reconstructions of the heat source.

Keywords: Heat equation, heat source, conjugate gradient method, inverse problem.

1 Introduction

Mathematical models related to inverse source problems arise in various practical settings, e.g. the determination of sources of water and air pollution in the environment, the determination of heat sources in heat conduction, etc. Consequently, inverse source problems for the heat equation have attracted considerable interest, see e.g. [3]–[8], [12], [17]–[19]. In all these studies the source function is sought as a function of either space or time. The reason for this restriction is the

lack of uniqueness of solution in the general case when the source depends on both space and time, [10]. That is why inverse problems for finding sources depending on various/several variables are of great interest. For example, it is possible to restore uniqueness if we seek the source as a linear combination of point sources, [1], or as an additive, [11], or multiplicative, [20], expression of separate time and space-dependent continuous components.

The objective of this paper is to determine heat source functions depending on both space and time, but which are the sum of two unknown components depending separately on space and time, with known weights depending on time and space, respectively. The additional measurements/overspecified conditions are given by integral observations of the temperature over space and time. This is particular advantageous in practical applications where local point or instant temperature measurements contain too large errors and then the use of non-local average measurements appears more realistic and reliable.

The inverse problem is linear, but ill-posed. The local existence and uniqueness of a classical solution in Hölder spaces are established in section 2, but more importantly this novel inverse formulation based on non-local average integral observations rather than local space or time point measurement enables the development of a weak solution theory for which variational methods are at hand, as developed in section 3. The discretization of the direct and adjoint problems is based on the finite element method (FEM) which is briefly discussed in section 4. The iterative conjugate gradient method (CGM) employed for minimizing the least-squares gap between the measured and computed data is also presented in section 4. As expected, since the solution of the inverse problem does not depend continuously on the input data, regularization needs to be enforced in order to obtain a stable solution. This is performed by either stopping the CGM iteration at a threshold given by the discrepancy principle, or by penalizing the least-squares functional with extra regularization terms. Numerical results obtained for several benchmark test examples are presented and discussed in section 5. Finally, section 6 gives the conclusions of the paper.

2 Mathematical Formulation

In this paper, we consider the particular practical application of the inverse analysis in the search of the heat source distribution in a multi-dimensional conductor. The determination of this heat source distribution across the space and time solution domain has a significant importance on finding the characteristics and performances of the thermal field. Further, it also assists in the designing of new heat conducting devices with an improved performance.

Let Ω be a bounded domain in $\mathbb{R}^n$ with boundary $\partial\Omega$, and T a given positive number. Denote $Q := \Omega \times (0, T]$, and $S := \partial\Omega \times (0, T]$. In [11], the problem of determining the right hand coefficients $f_1(x)$ and $f_2(t)$ in the Dirichlet problem

$$u_t = \Delta u + g_0(x,t) + f_1(x)g_1(t) + f_2(t)g_2(x), \quad (x,t) \in Q, \tag{2.1}$$

$$u|_{t=0} = u_0(x), \quad x \in \Omega, \tag{2.2}$$

$$u|_S = u_S, \tag{2.3}$$

from the two additional conditions

$$u(x_0,t)=h(t),\quad t\in[0,T], \tag{2.4}$$

$$\int_0^T u(x,t)dt=g(x),\quad x\in\bar{\Omega}, \tag{2.5}$$

where x_0 is a fixed point in Ω, has been considered. Based on the trivial identity $(f_1(x)+cg_2(x))g_1(t)+(f_2(t)-cg_1(t))g_2(x)=f_1(x)g_1(t)+f_2(t)g_2(x)$, where c is an arbitrary constant, one can see that problem (2.1)–(2.5) does not have a unique solution. However, if one imposes the additional condition that $f_1(x_0)$ is known then, under some conditions on the smoothness of the data and their compatibility, it can be established, see [11], that if T is small, then there exists a unique solution to the inverse problem. The aim of our paper is to solve this inverse source problem by a variational method. Since the pointwise measurement (2.4) cannot be defined in the usual weak form framework, we replace it by the integral measurement

$$l_1u:=\int_\Omega \omega_1(x)u(x,t)dx=h(t),\quad t\in(0,T), \tag{2.6}$$

where ω_1 is a given function.

We also assume that we have available as prescribed the quantity

$$\int_\Omega \omega_1(x)f_1(x)dx=C_0. \tag{2.7}$$

Then we have the following local uniqueness solvability theorem.

Theorem 2.1. *Suppose that the following conditions are satisfied:*

(A1) Equation (2.2) *holds for* $x\in\overline{\Omega}$, *equation* (2.3) *holds on* $\overline{S}$ *and equation* (2.6) *holds for* $t\in[0,T]$;

(A2) $u_0\in H^{2+\gamma}(\overline{\Omega}), g\in H^{2+\gamma}(\overline{\Omega}), u_s\in H^{2+\gamma,1+\gamma/2}(\overline{\Omega}), g_0\in H^{\gamma}(\overline{\Omega}), h\in H^{1+\gamma/2}[0,T], \omega_1\in H^{2+\gamma}(\Omega), \partial\Omega\in H^{2+\gamma}$, *where* $\gamma\in(0,1)$;

(A3) $u_0|_{\partial\Omega}=u_s(\cdot,0)|_{\partial\Omega}$, $g|_{\partial\Omega}=\int_0^T u_s(\cdot,t)|_{\partial\Omega}dt$, $h(0)=\int_\Omega \omega_1(x)u_0(x)dx$, $\int_\Omega \omega_1(x)g(x)dx=\int_0^T h(t)dt$;

(A4) $\int_0^T g_1(t)dt\neq 0$, $\int_\Omega \omega_1(x)g_2(x)dx\neq 0$, $g_1(t)/\int_0^T g_1(\tau)d\tau\geq 0, t\in[0,T]$.

Then for sufficiently small $T>0$ *there exists a unique solution* $(f_1,f_2,u)\in H^{\gamma}(\overline{\Omega})\times H^{\gamma/2}[0,T]\times H^{2+\gamma,1+\gamma/2}(\overline{Q})$ *of the inverse problem given by equations* (2.1)–(2.3) *and* (2.5)–(2.7).

For the definition of the above Hölder spaces involved, see [14, p. 7].

Proof. Differentiating (2.6) yields

$$\begin{aligned}h'(t)&=\int_\Omega \omega_1(x)u_t(x,t)dx=\int_\Omega \omega_1(x)\Big(\Delta u(x,t)+g_0(x,t)+f_1(x)g_1(t)+f_2(t)g_2(x)\Big)dx\\&=\int_\Omega\Big(u(x,t)\Delta\omega_1(x)+\omega_1(x)(g_0(x,t)+f_1(x)g_1(t))\Big)dx+f_2(t)\int_\Omega \omega_1(x)g_2(x)dx\\&\quad+\int_{\partial\Omega}\Big(\omega_1(x)\frac{\partial u}{\partial\nu}(x,t)-u_s(x,t)\frac{\partial\omega_1}{\partial\nu}(x,t)\Big)ds.\end{aligned}$$

Rearranging we obtain

$$f_2(t) = \frac{1}{\int_\Omega \omega_1(x)g_2(x)dx}\Big[h'(t) - \int_\Omega(\omega_1(x)g_0(x,t) + u(x,t)\Delta\omega_1(x))dx - C_0 g_1(t) + \int_{\partial\Omega}(u_s(x,t)\frac{\partial\omega_1}{\partial\nu}(x,t) - \omega_1(x)\frac{\partial u}{\partial\nu}(x,t))dS\Big], \quad t \in [0,T]. \tag{2.8}$$

Integrating (2.8) and using (2.5) we obtain

$$\begin{aligned}\int_0^T f_2(t)dt &= \frac{1}{\int_\Omega \omega_1(x)g_2(x)dx}\Big[h(T) - h(0) - \int_0^T\int_\Omega \omega_1(x)g_0(x,t)dxdt - \int_\Omega g(x)\Delta\omega_1(x)dx \\ &\quad - C_0\int_0^T g_1(t)dt + \int_{\partial\Omega}(g(x)\frac{\partial\omega_1}{\partial\nu}(x) - \omega_1(x)\frac{\partial g}{\partial\nu}(x))dS\Big] \\ &= \frac{1}{\int_\Omega \omega_1(x)g_2(x)dx}\Big[h(T) - h(0) - \int_Q \omega_1(x)g_0(x,t)dxdt \\ &\quad - \int_\Omega \omega_1(x)\Delta g(x)dx - C_0\int_0^T g_1(t)dt\Big] := F_1. \end{aligned} \tag{2.9}$$

We remark that F_1 is known from the data of the problem.

Taking the Laplacian of (2.5) yields

$$\begin{aligned}\Delta g(x) &= \int_0^T \Delta u(x,t)dt = \int_0^T (u_t(x,t) - g_0(x,t) - f_1(x)g_1(t) - f_2(t)g_2(x))dt \\ &= u(x,T) - u_0(x) - \int_0^T g_0(x,t)dx - f_1(x)\int_0^T g_1(t)dt - g_2(x)\int_0^T f_2(t)dt.\end{aligned}$$

Using (2.9) and rearranging we obtain

$$f_1(x) = \frac{1}{\int_0^T g_1(t)dt}\Big[u(x,T) - u_0(x) - \int_0^T g_0(x,t)dx - \Delta g(x) - g_2(x)F_1\Big], \quad x \in \overline{\Omega}. \tag{2.10}$$

Let $U_0 \in C^{2,1}(Q) \cap C^{1,0}(\overline{Q})$ be the solution of the direct problem (2.1) with $f_1 = f_2 = 0$ subject to (2.2) and (2.3). Then, if G is the Green function of the Dirichlet problem for the heat equation (2.1) with $f_1 = f_2 = g_0 = 0$, the solution $u(x,t)$ possesses the representation

$$u(x,t) = U_0(x,t) + \int_0^t\int_\Omega G(x,t;\xi,\tau)\Big(f_1(\xi)g_1(\tau) + f_2(\tau)g_2(\xi)\Big)d\xi d\tau, \quad (x,t) \in \overline{Q}. \tag{2.11}$$

Applying (2.11) for $t = T$ and substituting into (2.10) we obtain

$$f_1(x) = f_{01}(x) + \frac{1}{\int_0^T g_1(t)dt}\int_0^T\int_\Omega G(x,T;\xi,\tau)\Big(f_1(\xi)g_1(\tau) + f_2(\tau)g_2(\xi)\Big)d\xi d\tau, \quad x \in \overline{\Omega}, \tag{2.12}$$

where

$$\begin{aligned}f_{01}(x) &= \frac{1}{\int_0^T g_1(t)dt}\Big[U_0(x,T) - u_0(x) - \int_0^T g_0(x,t)dx - \Delta g(x) - F_1 g_2(x)\Big] \\ &= \frac{1}{\int_0^T g_1(t)dt}\Big[\int_0^T \Delta U_0(x,t)dt - \Delta g(x) - F_1 g_2(x)\Big], \quad x \in \overline{\Omega}\end{aligned} \tag{2.13}$$

is a known function from the data of the problem. Also, taking the gradient of (2.11) multiplied with the outward unit normal ν and substituting into (2.8) we obtain

$$f_2(t) = \frac{1}{\int_\Omega \omega_1(x)g_2(x)dx}\Big\{h'(t) - C_0 g_1(t) - \int_\Omega \omega_1(x)g_0(x,t)dx + \int_{\partial\Omega} u_s(x,t)\frac{\partial \omega_1}{\partial \nu}(x)dS$$
$$- \int_{\partial\Omega} \omega_1(x)\Big[\frac{\partial U_0}{\partial \nu}(x,t) + \int_0^t \int_\Omega \frac{\partial G}{\partial \nu_x}(x,t;\xi,\tau)(f_1(\xi)g_1(\tau) + f_2(\tau)g_2(\xi)\Big)d\xi d\tau\Big]dS_x$$
$$- \int_\Omega \Delta\omega_1(x)\Big[U_0(x,t) + \int_0^t \int_\Omega G(x,t;\xi,\tau)(f_1(\xi)g_1(\tau) + f_2(\tau)g_2(\xi))d\xi d\tau\Big]dx\Big\},$$

or

$$f_2(t) = f_{02}(t) - \frac{1}{\int_\Omega \omega_1(x)g_2(x)dx}\int_0^t \int_\Omega \Big(\int_\Omega \omega_1(x)\Delta_x G(x,t;\xi,\tau)dx\Big)$$
$$\times (f_1(\xi)g_1(\tau) + f_2(\tau)g_2(\xi))d\xi d\tau, \quad t \in [0,T], \tag{2.14}$$

where

$$f_{02}(t) = \frac{1}{\int_\Omega \omega_1(x)g_2(x)dx}\Big[h'(t) - C_0 g_1(t) - \int_\Omega \omega_1(x)g_0(x,t)dx + \int_{\partial\Omega} u_s(x,t)\frac{\partial \omega_1}{\partial \nu}(x)dS$$
$$- \int_{\partial\Omega} \omega_1(x)\frac{\partial U_0}{\partial \nu}(x,t)dS - \int_\Omega \Delta\omega_1(x)U_0(x,t)dx\Big]$$
$$= \frac{1}{\int_\Omega \omega_1(x)g_2(x)dx}\Big[h'(t) - C_0 g_1(t) - \int_\Omega \omega_1(x)\frac{\partial U_0}{\partial t}(x,t)dx\Big], \quad t \in [0,T] \tag{2.15}$$

is a known function from the data of the problem. Now the problem is equivalent to the coupled system of equations formed with the Fredholm integral equation (2.12) and the Volterra integral equation (2.14), and the functions $f_{01}(x)$ and $f_{02}(t)$ are known from the data of the problem. It is shown in [11] that the equation

$$f_1(x) = f_{01}(x) + \frac{1}{\int_0^T g_1(t)dt}\int_0^T \int_\Omega G(x,T;\xi,\tau)f_1(\xi)g_1(\tau)d\xi d\tau, \quad x \in \overline{\Omega},$$

has a unique solution which may be represented in terms of the resolvent $\Gamma(x,\xi)$. So, the function $f_1(x)$ can be expressed via the function $f_2(t)$ in the following way:

$$f_1(x) = \int_\Omega \Gamma(x,y)\Big(f_{01}(y) + \frac{1}{\int_0^T g_1(t)dt}\int_0^T \int_\Omega G(y,T;\xi,\tau)f_2(\tau)g_2(\xi)d\xi d\tau\Big)dy, \quad x \in \overline{\Omega}. \tag{2.16}$$

Introducing (2.16) into (2.14) gives the following integral equation with respect to $f_2(t)$:

$$f_1(t) = \widetilde{f_{02}}(t) - \frac{1}{\int_\Omega \omega_1(x)g_2(x)dx}\int_0^1 \int_\Omega \Big(\int_\Omega \omega_1(x)\Delta_x G(x,t;\xi,\tau)dx\Big)$$
$$\times f_2(\tau)g_2(\xi)d\xi d\tau - \frac{1}{\int_\Omega \omega_1(x)g_2(x)dx\int_0^T g_1(t)dt}\int_0^t \int_\Omega \Big(\int_\Omega \omega_1(x)\Delta_x G(x,t;\xi,\tau)dx\Big)$$
$$\times g_1(\tau)d\tau\Big[\int_\Omega \Gamma(\xi,y)\Big(\int_0^T \int_\Omega G(y,T;\eta,\sigma)g_2(\eta)f_2(\sigma)d\eta d\sigma\Big)dy\Big]d\xi, \quad t \in [0,T], \tag{2.17}$$

where

$$\widetilde{f_{02}}(t) = f_{02}(t) - \frac{1}{\int_\Omega \omega_1(x)g_2(x)dx}\int_0^1 \int_\Omega \Big(\int_\Omega \omega_1(x)\Delta_x G(x,t;\xi,\tau)dx\Big)$$
$$\times g_1(\tau)d\tau\Big(\int_\Omega \Gamma(\xi,y)f_{01}(y)dy\Big)d\xi, \quad t \in [0,T].$$

It is easy to see that the right-hand side of (2.17) is composed of two integral operators; one of them being a Volterra operator and another one a Fredholm operator. In summary, the equation (2.17) is of Fredholm type and, therefore, existence and uniqueness of solution for this equation are provided by the condition that the norm of its kernel is less than 1. From this condition, one may find the value of T_0 such that the equation (2.17), and the system (2.12), (2.14), in the whole, possesses a unique solution for $x \in \overline{\Omega}, t \in [0, T_0]$. □

In the above, we have already replaced the pointwise measurement (2.4) by the integral measurement (2.6). We also generalize (2.5) by replacing it with

$$l_2 u := \int_0^T \omega_2(t) u(x,t) dt = g(x), \quad x \in \Omega, \tag{2.18}$$

where ω_2 is a known function. Then we can formulate the inverse problem (2.1)–(2.3), (2.6), (2.7) and (2.18) in the weak sense as follows.

First, we suppose that the given data $g_0 \in L^2(Q), g_1 \in L^2(0,T), g_2 \in L^2(\Omega), u_0 \in L^2(\Omega), u_S \equiv 0, h \in L^2(0,T), g \in L^2(\Omega)$, $\omega_1 \in L^2(\Omega), \omega_2 \in L^2(0,T)$ are non-negative almost everywhere and $\int_\Omega \omega_1(x)dx > 0$, $\int_0^T \omega_2(t)dt > 0$. The sought functions f_1 and f_2 are supposed to be in $L^2(\Omega)$ and $L^2(0,T)$, respectively.

Note that if we formally take ω_1 and ω_2 as Dirac δ-like functions then this leads to approximate point-wise observations of u.

The solution of (2.1)–(2.3) with $u_S \equiv 0$ (this condition is for convenience only) is understood in the weak sense. Denote $F(x,t) := g_0(x,t) + f_1(x)g_1(t) + f_2(t)g_2(x)$. A function $u \in W(0,T) := \{u \in L^2(0,T; H_0^1(\Omega)), u_t \in L^2(0,T; H^{-1}(\Omega))\}$ is said to be a weak solution to (2.1)–(2.3), if it satisfies (2.2) and the identity

$$\int_0^T \langle u_t, \eta \rangle_{(H^{-1}(\Omega), H_0^1(\Omega))} dt = -\int_Q \nabla u \cdot \nabla \eta dx dt + \int_Q F\eta dx dt, \quad \forall \eta \in L^2(0,T; H_0^1(\Omega)). \tag{2.19}$$

Here $H^1(\Omega)$ and $H_0^1(\Omega)$ are standard Sobolev spaces. It can be proved [2, Theorems 2, 3, pp. 354–357] (or [21]) that there exists a unique weak solution of (2.1)–(2.3), and furthermore, there exists a constant c independent of F and u_0 such that

$$\|u\|_{W(0,T)} \le c(\|F\|_{L^2(Q)} + \|u_0\|_{L^2(\Omega)}). \tag{2.20}$$

Since $W(0,T)$ is compactly embedded into $L^2(Q)$, the mapping $(f_1, f_2) \in L^2(\Omega) \times L^2(0,T) \to (l_1 u, l_2 u) \in L^2(0,T) \times L^2(\Omega)$ is compact. Therefore, the inverse problem (2.1)–(2.3), (2.6), (2.7) and (2.18) is ill-posed.

Consider the adjoint problem

$$-\psi_t = \Delta\psi + G(x,t), \quad (x,t) \in Q, \tag{2.21}$$

$$\psi(x,T) = \psi_T(x), \quad x \in \Omega, \tag{2.22}$$

$$\psi|_S = 0, \tag{2.23}$$

with $G \in L^2(Q)$ and $\psi_T \in L^2(\Omega)$. The solution of this adjoint problem is also understood in the weak sense as above and it is known, [2, Theorems 2, 3, pp. 354–357], that there exists a unique solution $\psi \in W(0,T)$, and there exists also a constant c' such that

$$\|\psi\|_{W(0,T)} \le c'(\|G\|_{L^2(Q)} + \|\psi_T\|_{L^2(\Omega)}). \tag{2.24}$$

Furthermore, the following Green formula is valid [21]:

$$\int_\Omega u_0(x)\eta(x,0)dx + \int_Q F\psi dxdt = \int_\Omega u(x,T)\psi_T(x)dx + \int_Q Gudxdt. \tag{2.25}$$

We are now ready to introduce the least-squares method for solving the inverse problem (2.1)–(2.3), (2.6), (2.7) and (2.18).

3 Variational Method

Denote the solution of (2.1)–(2.3) by $u(x,t;f) = u(x,t;f_1,f_2) = u(f)$, where $f = (f_1,f_2)$. The variational method for solving the inverse problem of determining f_1 and f_2 from (2.1)–(2.3), (2.6), (2.7) and (2.18) minimizes the functional

$$\begin{aligned} J_\alpha(f) = \frac{1}{2}\|l_1u(f)-h\|^2_{L^2(0,T)} + \frac{1}{2}\|l_2u(f)-g\|^2_{L^2(\Omega)} + \frac{1}{2}\Big(\int_\Omega \omega_1(x)f_1(x)dx - C_0\Big)^2 \\ + \frac{\alpha_1}{2}\|f_1\|^2_{L^2(\Omega)} + \frac{\alpha_2}{2}\|f_2\|^2_{L^2(0,T)}, \end{aligned} \tag{3.1}$$

with $\alpha_1,\alpha_2 \geq 0$ being the regularization parameters, $\alpha = (\alpha_1,\alpha_2)$, over $L^2(\Omega)\times L^2(0,T)$. We take the convention that if $\alpha_1 = \alpha_2$, then we simply denote them by α.

Now we prove that J_α is Fréchet differentiable and derive its gradient formula.

Let $\delta f := (\delta f_1,\delta f_2) \in L^2(\Omega)\times L^2(0,T)$ be a variation of f. Denoting by $\delta u = u(f+\delta f) - u(f)$, we see that it satisfies the system

$$\delta u_t = \Delta\delta u + \delta f_1(x)g_1(t) + \delta f_2(t)g_2(x), \quad (x,t)\in Q, \tag{3.2}$$

$$\delta u|_{t=0} = 0, \quad x\in\Omega, \tag{3.3}$$

$$\delta u|_S = 0. \tag{3.4}$$

It is clear that there exists a unique solution in $W(0,T)$ of this problem and, see [2, Theorems 2, 3, pp. 354–357],

$$\|\delta u\|_{W(0,T)} \leq c\big(\|\delta f_1(\cdot)g_1(\cdot)\|_{L^2(Q)} + \|\delta f_2(\cdot)g_2(\cdot)\|_{L^2(Q)}\big). \tag{3.5}$$

We have

$$\begin{aligned} J_0(f+\delta f) - J_0(f) =& \langle l_1\delta u, l_1u(f)-h\rangle_{L^2(0,T)} + \langle l_2\delta u, l_2u(f)-g\rangle_{L^2(\Omega)} \\ &+ <\omega_1,\delta f_1>_{L^2(\Omega)} (<\omega_1,f_1>_{L^2(\Omega)} - C_0) \\ &+ \frac{1}{2}\|l_1\delta u\|^2_{L^2(0,T)} + \frac{1}{2}\|l_2\delta u\|^2_{L^2(\Omega)} + \frac{1}{2}<\omega_1,\delta f_1>^2_{L^2(\Omega)} \\ =& \int_Q \omega_1(x)\big(l_1u(f)-h(t)\big)\delta u dxdt + \int_Q \omega_2(t)\big(l_2u(f)-g(x)\big)\delta u dxdt \\ &+ \Big(\int_\Omega \omega_1(x)\delta f_1(x)dx\Big)\Big(\int_\Omega \omega_1(x)f_1(x)dx - C_0\Big) \\ &+ \frac{1}{2}\|l_1\delta u\|^2_{L^2(0,T)} + \frac{1}{2}\|l_2\delta u\|^2_{L^2(\Omega)} + \frac{1}{2}<\omega_1,\delta f_1>^2_{L^2(\Omega)}. \end{aligned}$$

Consider the adjoint problem

$$-\psi_t = \Delta\psi + \omega_1(x)\big(l_1u(f) - h(t)\big) + \omega_2(t)\big(l_2u(f) - g(x)\big), \quad (x,t) \in Q, \tag{3.6}$$

$$\psi(x,T) = 0, \quad x \in \Omega, \tag{3.7}$$

$$\psi|_S = 0, \tag{3.8}$$

The function $\psi \in W(0,T)$ and from the Green formula (2.25) we obtain

$$\int_Q \Big(\delta f_1(x)g_1(t) + \delta f_2(t)g_2(x)\Big)\psi(x,t)dxdt$$
$$= \int_Q \Big(\omega_1(x)\big(l_1u(f) - h(t)\big) + \omega_2(t)\big(l_2u(f) - g(x)\big)\Big)\delta u dxdt.$$

Hence

$$J_0(f+\delta f) - J_0(f) = \int_Q \Big(\delta f_1(x)g_1(t) + \delta f_2(t)g_2(x)\Big)\psi(x,t)dxdt$$
$$+ \Big(\int_\Omega \omega_1(x)\delta f_1(x)dx\Big)\Big(\int_\Omega \omega_1(x)f_1(x)dx - C_0\Big)$$
$$+ \frac{1}{2}\|l_1\delta u\|^2_{L^2(0,T)} + \frac{1}{2}\|l_2\delta u\|^2_{L^2(\Omega)} + \frac{1}{2} < \omega_1, \delta f_1 >^2_{L^2(\Omega)} .$$

Due to the a priori estimate (2.20)

$$\|l_1\delta u\|^2_{L^2(0,T)} + \|l_2\delta u\|^2_{L^2(\Omega)} = o(\|\delta f_1\|_{L^2(\Omega)} + \|\delta f_2\|_{L^2(0,T)}).$$

It follows that J_0 is Fréchet differentiable and its gradient has the form

$$J_0'(f) = \Big\{\int_0^T g_1(t)\psi(x,t)dt + \Big(\int_\Omega \omega_1(x)f_1(x)dx - C_0\Big)\omega_1(x), \int_\Omega g_2(x)\psi(x,t)dx\Big\}. \tag{3.9}$$

Thus, J_α is also Fréchet differentiable and its gradient has the form

$$J_\alpha'(f) = \Big\{\int_0^T g_1(t)\psi(x,t)dt + \Big(\int_\Omega \omega_1(x)f_1(x)dx - C_0\Big)\omega_1(x) + \alpha_1 f_1(x),$$
$$\int_\Omega g_2(x)\psi(x,t)dx + \alpha_2 f_2(t)\Big\}. \tag{3.10}$$

Since we minimize J_α in the whole space $L^2(\Omega) \times L^2(0,T)$, the optimal solution satisfies

$$\int_0^T g_1(t)\psi(x,t)dt + \Big(\int_\Omega \omega_1(x)f_1(x)dx - C_0\Big)\omega_1(x) + \alpha_1 f_1(x) = 0, \tag{3.11}$$

$$\int_\Omega g_2(x)\psi(x,t)dx + \alpha_2 f_2(t) = 0. \tag{3.12}$$

4 The Conjugate Gradient Method

First, we shall discretize the variational problem of the previous section by the FEM and prove some convergence results. We do not use the boundary element method (BEM) because we want to allow, if necessary, for a spacewise-dependent thermal conductivity $k(x) > 0$ material, i.e. we can replace the Laplacian term Δu in (2.1) by the term $\nabla \cdot (k(x)\nabla u)$.

To this end, we suppose that Ω is a polyhedral domain and $u_0 \in H_0^1(\Omega)$. We note that when $u_0 \in H_0^1(\Omega)$, the solution $u \in W(0,T)$ to (2.1)–(2.3) belongs to $L^2(0,T;H^2(\Omega)) \cap H^1(0,T;L^2(\Omega)) \hookrightarrow C(0,T;H^1(\Omega))$, see [2, Theorem 5, pp. 360–361].

We triangulate Ω into a shape regular quasi-uniform mesh $\mathcal{T}_\mathrm{h}$ of simplicial elements and then define the piecewise linear finite element space $V_\mathrm{h} \subset H_0^1(\Omega)$ by

$$V_\mathrm{h} = \{v_\mathrm{h} : v_\mathrm{h} \in C(\overline{\Omega}), v_\mathrm{h}|_K \in P_1(K), \forall K \in \mathcal{T}_\mathrm{h}\}, \tag{4.1}$$

where $P_1(K)$ is the space of linear polynomials on the element K. To fully discretize (2.1)–(2.3) we introduce a uniform partition of the interval $[0,T] : 0 = t_0 < t_1 < \cdots < t_N = T$, where $\tau = T/N$ is the temporal step size and $t_k = k\tau$ for $k = 0, 1, \ldots, N$, are the partition points. For a sequence $\{w^k\}, k = 0, 1, \ldots, N$, denote by $\bar{w}_{\mathrm{h},\tau}$ its piecewise constant interpolant, i.e., for $t \in (t_{k-1}, t_k), k = 1, \ldots, N$, $\bar{w} = w^k$. We denote this space by W_τ.

Now we discretize problem (2.1)–(2.3) by the Crank-Nicolson-FEM as follows: Find $u_\mathrm{h}^k \in V_\mathrm{h}$ for $k = 1, 2, ..., N$ such that

$$\left\langle \frac{u_\mathrm{h}^k - u_\mathrm{h}^{k-1}}{\tau}, v \right\rangle_{L^2(\Omega)} + \left\langle \nabla \frac{u_\mathrm{h}^k + u_\mathrm{h}^{k-1}}{2}, \nabla v \right\rangle_{L^2(\Omega)} = \left\langle \frac{F(\cdot,t_k) + F(\cdot,t_{k-1})}{2}, v \right\rangle_{L^2(\Omega)},$$

$$\forall v \in V_\mathrm{h}, k = 1, ..., N, \tag{4.2}$$

$$< u_\mathrm{h}^0, v >_{L^2(\Omega)} =< u_0, v >_{L^2(\Omega)}, \quad \forall v \in V_\mathrm{h}. \tag{4.3}$$

Denote by $\bar{u}_{\mathrm{h},\tau}$ the piecewise constant interpolant of $\{u_\mathrm{h}^k\}$. It is standard that (see e.g., [13]) $\|\bar{u}_{\mathrm{h},\tau} - u\|_{L^2(Q)} \le c(\tau + \mathrm{h}^2)$.

Suppose that h and g are approximately given by $h_{\delta_1} \in L^2(0,T)$ and $g_{\delta_2} \in L^2(\Omega)$, respectively:

$$\|h - h_{\delta_1}\|_{L^2(0,T)} \le \delta_1, \quad \|g - g_{\delta_2}\|_{L^2(\Omega)} \le \delta_2. \tag{4.4}$$

If $\delta_1 = \delta_2$, we simply denote them by δ.

The discretized version of (3.1) has the form

$$J_{\mathrm{h},\tau,\alpha}(f_{\mathrm{h},\tau}) = \frac{1}{2}\|l_1\bar{u}_{\mathrm{h},\tau}(f_{\mathrm{h},\tau}) - h_{\delta_1}\|^2_{L^2(0,T)} + \frac{1}{2}\|l_2\bar{u}_{\mathrm{h},\tau}(f_{\mathrm{h},\tau}) - g_{\delta_2}\|^2_{L^2(\Omega)}$$
$$+ \frac{1}{2}\Big(\int_\Omega \omega_1(x) f_{1\mathrm{h}}(x)dx - C_0\Big)^2 + \frac{\alpha_1}{2}\|f_{1\mathrm{h}}\|^2_{L^2(\Omega)} + \frac{\alpha_2}{2}\|\bar{f}_{2\tau}\|^2_{L^2(0,T)}. \tag{4.5}$$

We shall minimize this functional over $V_\mathrm{h} \times W_\tau$. It is easily seen that this optimization problem has a unique solution $(f_{1\mathrm{h}}^*, f_{2\tau}^*)$ if $\alpha_1, \alpha_2 > 0$. Furthermore, if $\alpha_1 = \alpha_2 := \alpha > 0$, $\delta_1 = \delta_2 := \delta \ge 0$, denoting the solution of the minimizing the functional (3.1) by (f_1^*, f_2^*), we have

$$\|f_1^* - f_{1h}^*\|_{L^2(\Omega)} + \|f_2^* - f_{2\tau}^*\|_{L^2(0,T)} \le c\frac{1}{\alpha}(\tau + \mathrm{h} + \delta) \tag{4.6}$$

for some positive constant c . The proof of this inequality directly follows from [9] or [6], therefore, we do not present it here.

At this stage, it is useful and timely to give the algorithmic implementation of the iterative CGM, [5], which runs as follows.

1. Initialization

1.1 Choose an initial guess $f_0 = (f_{0,1}, f_{0,2}) \in L^2(\Omega) \times L^2(0,T)$.

1.2 Calculate the residual

$$\tilde{r}_0 = \begin{pmatrix} \tilde{r}_{0,1}(t) \\ \tilde{r}_{0,2}(x) \\ \tilde{r}_{0,3} \end{pmatrix} = \begin{pmatrix} l_1 u - h_{\delta_1} \\ l_2 u - g_{\delta_2} \\ l_3 f - C_0 \end{pmatrix} = \begin{pmatrix} \int\limits_\Omega \omega_1(x) u^0(x,t)dx - h_{\delta_1}(t) \\ \int\limits_0^T \omega_2(t) u^0(x,t)dt - g_{\delta_2}(x) \\ \int\limits_\Omega \omega_1(x) f_1(x)dx - C_0 \end{pmatrix}$$

by solving

$$\begin{cases} u^0_t = \Delta u^0 + g_0(x,t) + f_{0,1}(x) g_1(t) + f_{0,2}(t) g_2(x), \quad (x,t) \in Q, \\ u^0|_{t=0} = u_0(x), \quad x \in \Omega, \\ u^0|_S = u_S. \end{cases}$$

1.3 Calculate $J_\alpha(f_0) = \frac{1}{2}\|\tilde{r}_0\|^2 + \frac{\alpha_1}{2}\|f_{0,1}\|^2 + \frac{\alpha_2}{2}\|f_{0,2}\|^2$,
where

$$\|\tilde{r}_0\|^2 = \|\tilde{r}_{0,1}\|^2_{L^2(0,T)} + \|\tilde{r}_{0,2}\|^2_{L^2(\Omega)} + \tilde{r}^2_{0,3}.$$

1.4 Calculate the gradient r_0

$$r_0 = \begin{pmatrix} r_{0,1}(x) \\ r_{0,2}(t) \end{pmatrix} = \begin{pmatrix} \int\limits_0^T g_1(t)\psi^0(x,t)dt + \alpha_1 f_{0,1}(x) + \left(\int\limits_\Omega \omega_1(\xi) f_{0,1}(\xi) d\xi - C_0 \right) \omega_1(x) \\ \int\limits_\Omega g_2(x)\psi^0(x,t)dx + \alpha_2 f_{0,2}(t) \end{pmatrix}$$

by solving

$$\begin{cases} -\psi^0_t = \Delta \psi^0 + \omega_1(x)\tilde{r}_{0,1}(t) + \omega_2(t)\tilde{r}_{0,2}(x), \quad (x,t) \in Q, \\ \psi^0(x,T) = 0, \quad x \in \Omega, \\ \psi^0|_S = 0. \end{cases}$$

1.5 Define $d_0 = -r_0 = \begin{pmatrix} d_{0,1}(x) \\ d_{0,2}(t) \end{pmatrix}$.

2. For $n = 0, 1, 2, ...$

2.1 Solve

$$\begin{cases} u^n_t = \Delta u^n + d_{n,1}(x) g_1(t) + d_{n,2}(t) g_2(x), \quad (x,t) \in Q, \\ u^n|_{t=0} = 0, \quad x \in \Omega, \\ u^n|_S = 0 \end{cases}$$

and calculate $A_0 d_n = \begin{pmatrix} \int\limits_\Omega \omega_1(x) u^n(x,t)dx \\ \int\limits_0^T \omega_2(t) u^n(x,t)dt \\ \int\limits_\Omega \omega_1(x) f_1(x)dx \end{pmatrix} := \begin{pmatrix} A_{0,1}d_n \\ A_{0,2}d_n \\ A_{0,3}d_n \end{pmatrix}$. Then calculate

$$\beta_n = -\frac{(A_{0,3}d_n)\tilde{r}_{n,3} + \langle d_{n,1}, r_{n,1} \rangle_{L^2(\Omega)} + \langle d_{n,2}, r_{n,2} \rangle_{L^2(0,T)}}{\|A_0 d_n\|^2 + \alpha_1 \|d_{n,1}\|^2_{L^2(\Omega)} + \alpha_2 \|d_{n,2}\|^2_{L^2(0,T)}},$$

where

$$\|A_0 d_n\|^2 = \|A_{0,1} d_n\|^2_{L^2(0,T)} + \|A_{0,2} d_n\|^2_{L^2(\Omega)} + |A_{0,3} d_n|^2.$$

2.2 Update $f_{n+1} = f_n + \beta_n d_n$.

2.3 Calculate the residual $\tilde{r}_{n+1} = \tilde{r}_n + \beta_n A_0 d_n$.

2.4 Calculate the gradient r_{n+1}

$$r_{n+1} = \begin{pmatrix} r_{n+1,1}(x) \\ r_{n+1,2}(t) \end{pmatrix} = \begin{pmatrix} \int_0^T g_1(t)\psi^{n+1}(x,t)dt + \alpha_1 f_{n+1,1}(x) + \left(\int_\Omega \omega_1(\xi) f_{n+1,1}(\xi) d\xi - C_0 \right) \omega_1(x) \\ \int_\Omega g_2(x)\psi^{n+1}(x,t)dx + \alpha_2 f_{n+1,2}(t) \end{pmatrix}$$

by solving

$$\begin{cases} -\psi_t^{n+1} = \Delta\psi^{n+1} + \omega_1(x)\tilde{r}_{n+1,1}(t) + \omega_2(t)\tilde{r}_{n+1,2}(x), \quad (x,t) \in Q, \\ \psi^{n+1}(x,T) = 0, \quad x \in \Omega, \\ \psi^{n+1}|_S = 0. \end{cases}$$

2.5 Calculate $J_\alpha(f_{n+1}) = \frac{1}{2}\|\tilde{r}_{n+1}\|^2 + \frac{\alpha_1}{2}\|f_{n+1,1}\|^2_{L^2(0,T)} + \frac{\alpha_2}{2}\|f_{n+1,2}\|^2_{L^2(\Omega)}$, where

$$\|\tilde{r}_n\|^2 = \|\tilde{r}_{n,1}\|^2_{L^2(0,T)} + \|\tilde{r}_{n,2}\|^2_{L^2(\Omega)} + \tilde{r}^2_{n,3}.$$

2.6 Calculate $\gamma_n = \frac{\|r_{n+1}\|^2}{\|r_n\|^2}$.

2.7 Update $d_{n+1} = -r_{n+1} + \gamma_n d_n$.

For $\alpha = 0$, we stop the iteration procedure if $\|\tilde{r}_n\| \le \sigma\sqrt{\delta_1^2 + \delta_2^2}$, where $\sigma = 1.1$. It is well-known that such a stopping criterion has a regularization effect, [15, 16].

5 Numerical Examples and Discussion

An important feature of our analysis is that is valid in any dimension. Consequently, we illustrate typical numerical results for two-dimensional time-dependent solution domains. For the following three numerical examples, we choose $T = 1, \Omega = (0,1) \times (0,1)$,

$$u(x,t) = 1 - e^{x_1^2 + x_2}\cos(2t), \quad \omega_1(x) = 1, \quad \omega_2(t) = 1,$$
$$u_t - \Delta u = 2e^{x_1^2+x_2}\sin(2t) + (3 + 4x_1^2)e^{x_1^2+x_2}\cos(2t) = g_0(x,t) + f_1(x)g_1(t) + f_2(t)g_2(x),$$
$$g_1(t) = 2 + \sin(2t), \quad g_2(x) = (3 + 4x_1^2)e^{x_1^2+x_2},$$

where $x = (x_1, x_2)$. This generates the input data (2.2), (2.3), (2.6), and (2.18) given by

$$u_0(x) = 1 - e^{x_1^2+x_2}, \quad x \in \Omega,$$
$$u_S(x,t) = 1 - e^{x_1^2+x_2}\cos(2t), \quad (x,t) \in S,$$
$$h(t) = 1 + \frac{\sqrt{\pi}}{2}(1-e)\cos(2t)\mathrm{erfi}(1), \quad t \in (0,1),$$
$$g(x) = 1 - e^{x_1^2+x_2}\sin(2)/2, \quad x \in \Omega,$$

$\delta_1 = \delta_2$	n^*	$\|f_1 - f_{1n^*}\|_{L^2(\Omega)}$	$\|f_2 - f_{2n^*}\|_{L^2(0,T)}$	$J_0(f_{n*})$
5×10^{-4}	101	0.0390	0.0122	3.01E-7
10^{-3}	56	0.0432	0.0160	1.14E-6
10^{-2}	9	0.4887	0.0415	1.18E-4

Table 1: The results for Example 1 with noise.

where erfi is the imaginary error function. One can easily check that the conditions of Theorem 2.1 are satisfied such the the local existence and uniqueness of a classical solution are ensured.

The FEM is applied, as described in section 4, using the time step size $\tau = T/N = 1/N$ with $N = 32$ and the space mesh composed of $M = 4096$ finite elements. The initial guess for the initialization of the CGM was taken as $f_0 = (f_{01}(x), f_{02}(t)) = (0, 0)$. In the case of no noise, we select some values for the regularization parameters α_1 and α_2 and run the CGM until convergence is achieved. In fact, for no noise, in order to illustrate typical results we present them as those obtained after 500 iterations which was found sufficiently large to capture all the essential features of the numerical solution and do not increase the computational time beyond purpose. In the case of noisy data we take $\alpha_1 = \alpha_2 = 0$ and stop the CGM at the first iteration number n^* for which the stopping criterion

$$\|\tilde{r}_{n^*}\| \leq 1.1\sqrt{\delta_1^2 + \delta_2^2} \tag{5.1}$$

is satisfied. We test the stability of the numerical solution for various amounts of noise $\delta_1 = \delta_2 \in \{5 \times 10^{-4}, 10^{-3}, 10^{-2}\}$.

Example 1. The exact solution is

$$f_1(x) = \sin(2\pi x_1)\sin(3\pi x_2), \quad f_2(t) = \sin(2\pi t). \tag{5.2}$$

Then $C_0 = 0$. In this example, both functions f_1 and f_2 are smooth.

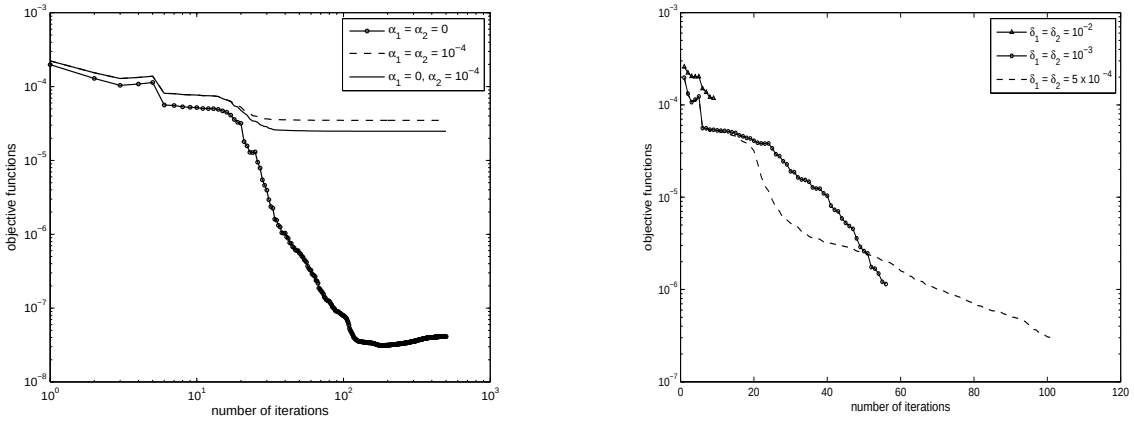

Figure 1: The objective functions without noise (left) and with noise (right) for Example 1.

Example 2. The exact solution is

$$f_1(x) = \sin(2\pi x_1)\sin(3\pi x_2), \quad f_2(t) = \begin{cases} 1 & \text{if } t \in [1/3, 2/3], \\ 0 & \text{otherwise.} \end{cases} \tag{5.3}$$

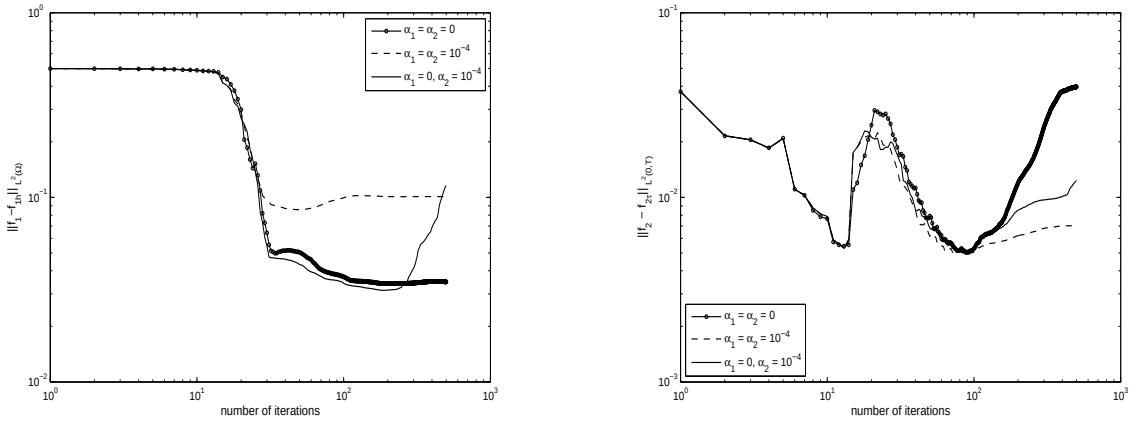

Figure 2: The errors $\|f_1 - f_{1\mathrm{h}}\|_{L^2(\Omega)}$ (left) and $\|f_2 - f_{2\tau}\|_{L^2(0,T)}$ (right) without noise for Example 1.

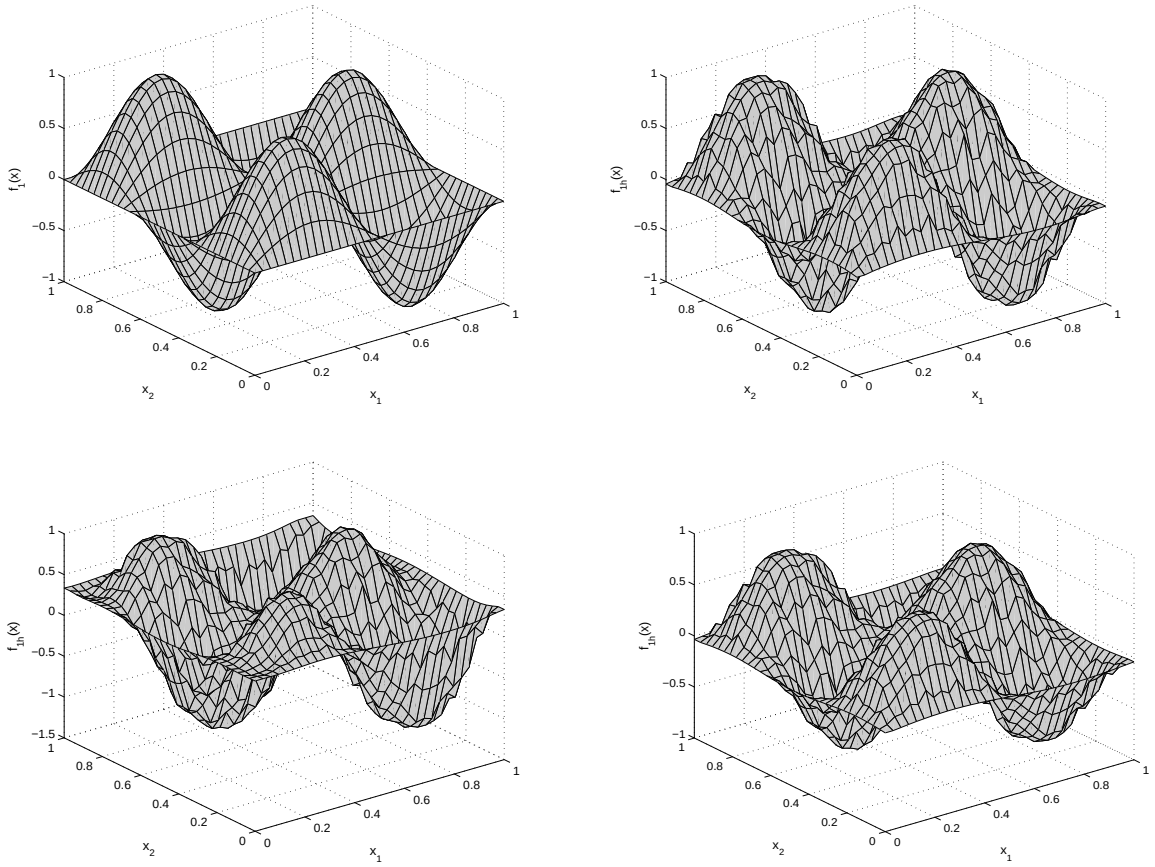

Figure 3: The exact solution $f_1(x)$ (top left) and the approximate solutions $f_{1\mathrm{h}}(x)$ without noise obtained with $\alpha_1 = \alpha_2 = 0$ (top right), $\alpha_1 = \alpha_2 = 10^{-4}$ (bottom left), and $\alpha_1 = 0, \alpha_2 = 10^{-4}$ (bottom right), for Example 1.

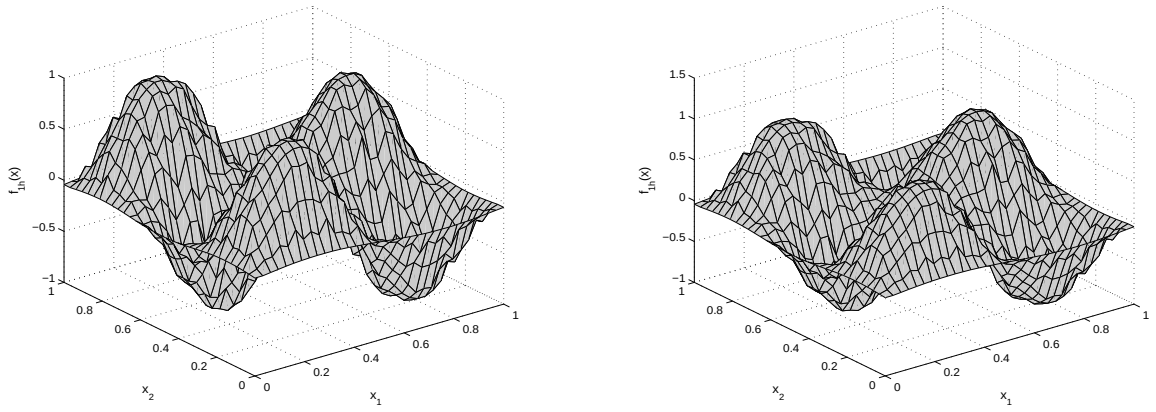

Figure 4: The approximate solutions $f_{1\mathrm{h}}(x)$ with noise $\delta_1 = \delta_2 = 5 \times 10^{-4}$ (left) and $\delta_1 = \delta_2 = 10^{-3}$ (right) for Example 1.

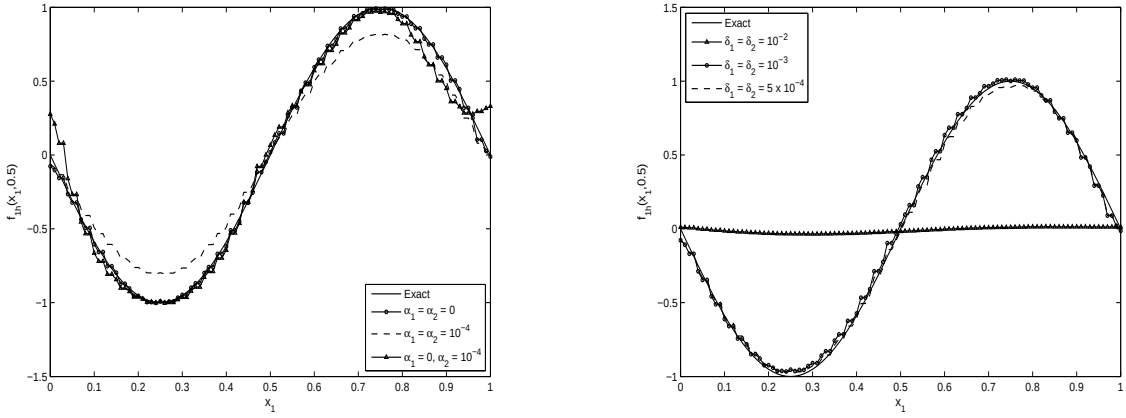

Figure 5: The approximate solutions $f_{1\mathrm{h}}(x_1, 0.5)$ without noise (left) and with noise (right) for Example 1.

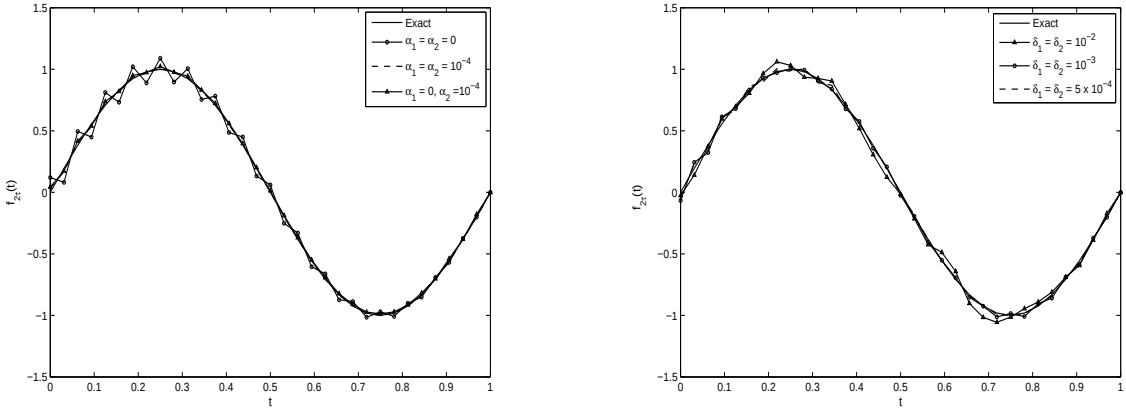

Figure 6: The approximate solutions $f_{2\tau}(t)$ without noise (left) and with noise (right) for Example 1.

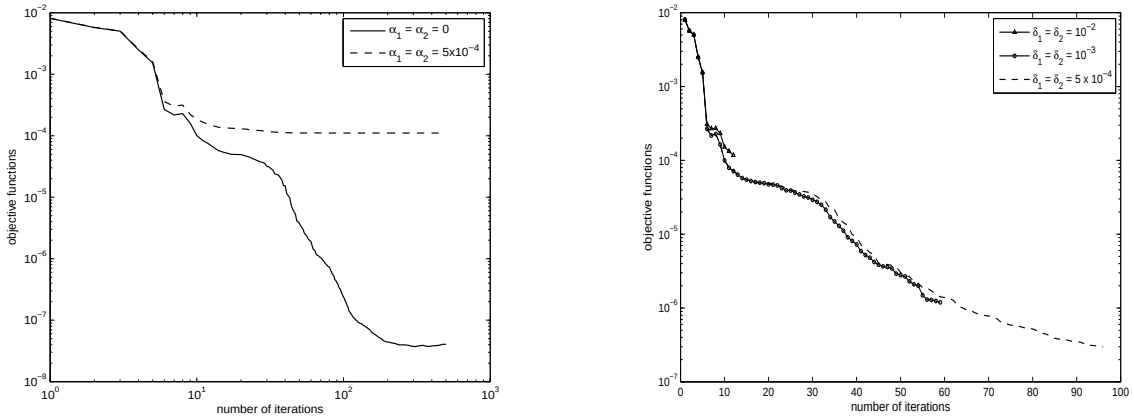

Figure 7: The objective functions without noise (left) and with noise (right) for Example 2.

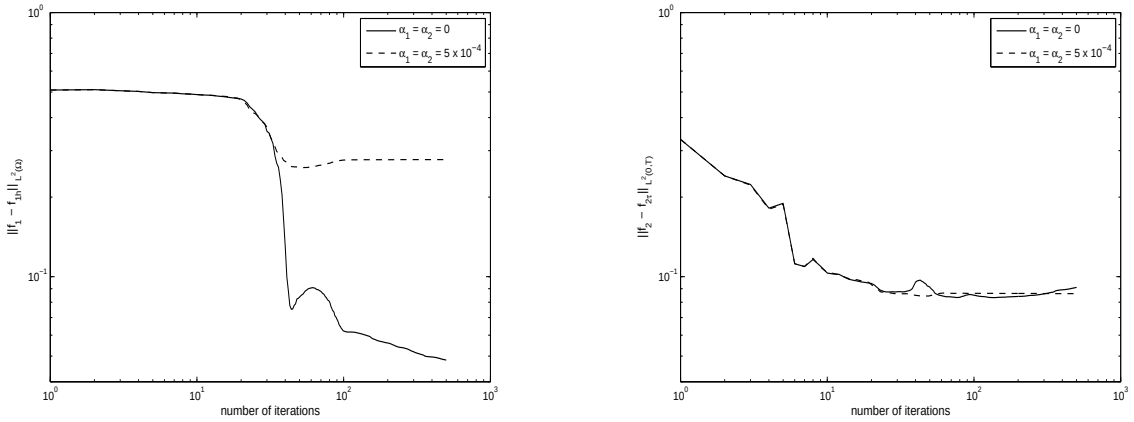

Figure 8: The errors $\|f_1 - f_{1\mathrm{h}}\|_{L^2(\Omega)}$ (left) and $\|f_2 - f_{2\tau}\|_{L^2(0,T)}$ (right) without noise for Example 2.

$\delta_1 = \delta_2$	n^*	$\|f_1 - f_{1n^*}\|_{L^2(\Omega)}$	$\|f_2 - f_{2n^*}\|_{L^2(0,T)}$	$J_0(f_{n*})$
5×10^{-4}	96	0.0687	0.0831	2.9E-7
10^{-3}	59	0.0702	0.0848	1.1E-6
10^{-2}	12	0.4870	0.1066	1.10E-4

Table 2: The results for Example 2 with noise.

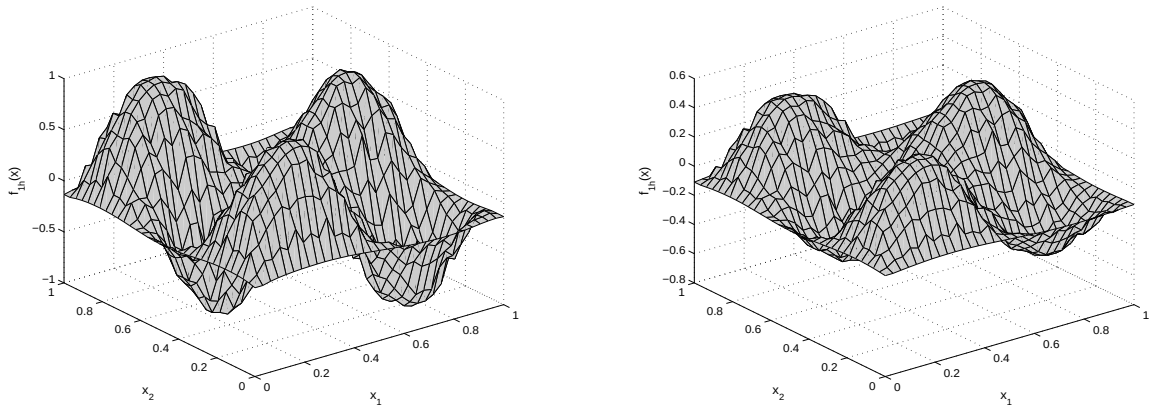

Figure 9: The approximate solutions $f_{1\mathrm{h}}(x)$ without noise obtained with $\alpha_1 = \alpha_2 = 0$ (left) and $\alpha_1 = \alpha_2 = 5 \times 10^{-4}$ (right) for Example 2.

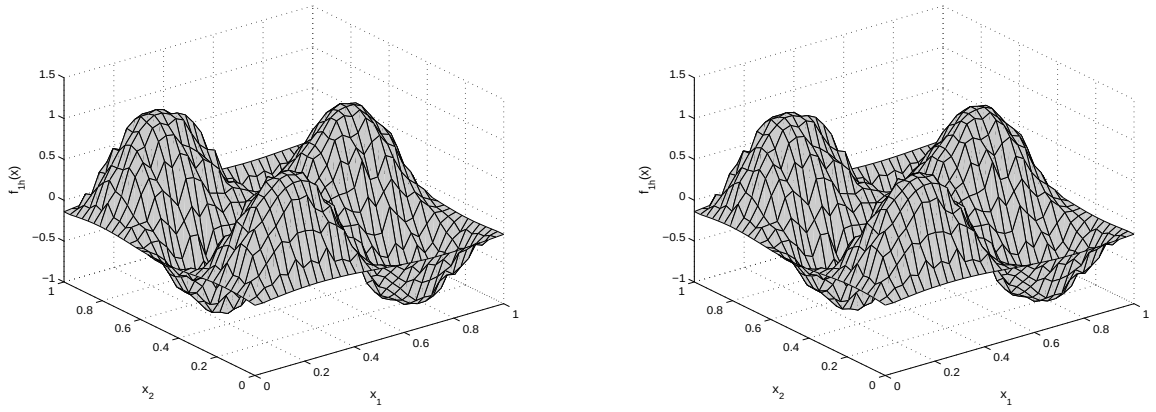

Figure 10: The approximate solutions $f_{1\mathrm{h}}(x)$ with noise: $\delta_1 = \delta_2 = 5 \times 10^{-4}$ (left) and $\delta_1 = \delta_2 = 10^{-3}$ (right) for Example 2.

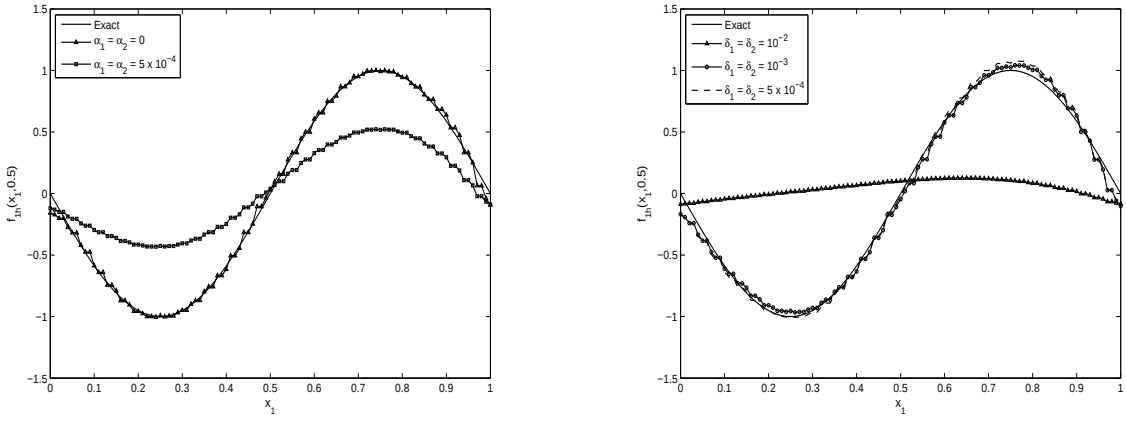

Figure 11: The approximate solutions $f_{1\mathrm{h}}(x_1, 0.5)$ without noise (left) and with noise $\alpha_1 = \alpha_2 = 0$ (right) for Example 2.

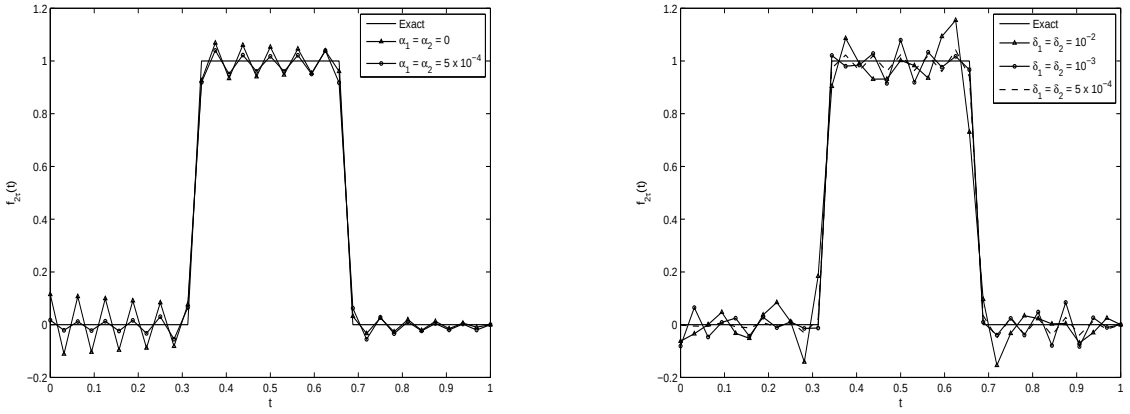

Figure 12: The approximate solutions $f_{2\tau}(t)$ without noise (left) and with noise (right) for Example 2.

Then $C_0 = 0$. In this example, the function f_1 is smooth, but f_2 is discontinuous.

Example 3. The exact solution is

$$f_1(x) = \begin{cases} 1 & \text{if } x \in [0.3, 0.7]^2, \\ 0 & \text{otherwise,} \end{cases} \qquad f_2(t) = \begin{cases} 1 & \text{if } t \in [1/3, 2/3], \\ 0 & \text{otherwise.} \end{cases} \tag{5.4}$$

Then $C_0 = 0.16$. In this example, both functions f_1 and f_2 are discontinuous.

5.1 Input Data Without Noise

We consider first the case of exact data, i.e. the input data (2.6) and (2.18) is without noise $\delta_1 = \delta_2 = 0$.

The objective function (3.1) is plotted, as a function of the number of iterations, in the left hand sides of Figures 1, 7 and 13 for Examples 1–3, respectively. Both cases of with, i.e. $\alpha \neq 0$, and without, i.e. $\alpha = 0$, regularization terms in (3.1) are illustrated. First, from these figures it can be seen that for $\alpha \neq 0$, the objective function J_α rapidly decreases and settles at a stationary value in about 20 iterations, showing that convergence has been achieved. Secondly, especially from the left hand side of Figure 1 it can be seen that for $\alpha = 0$ the objective function J_0 rapidly decreases for the first 100 iterations after which it starts increasing showing a semi-convergence phenomenon. This is expected since although we have no noisy random errors in the input data (2.6) and (2.18), because we input the analytical values for $g(x)$ and $h(t)$, there will still exist a numerical "noise" generated by the use of a numerical discretization method with a fixed finite mesh size.

The behaviour of the errors $\|f_1 - f_{1\mathrm{h}}\|_{L^2(\Omega)}$ and $\|f_2 - f_{2\tau}\|_{L^2(0,T)}$, as functions of the number of iterations, are shown in Figures 2, 8 and the right-hand side of Figures 13 for Examples 1–3, respectively. From these figures it can be seen that for $\alpha = 0$, after about 100 iterations the errors $\|f_1 - f_{1\mathrm{h}}\|_{L^2(\Omega)}$ decrease, whilst the errors $\|f_2 - f_{2\tau}\|_{L^2(0,T)}$ increase. On the other hand, we can reverse this behaviour by including some regularization. This reveals an interesting balancing phenomenon happening in the sum of the sources in (2.1), namely, increasing the accuracy in $f_1(x)$ results in decreasing the accuracy in $f_2(t)$ and vice versa.

The numerical solutions $f_{1\mathrm{h}}(x_1, x_2)$ are shown in comparison with the exact solutions $f(x_1, x_2)$ in Figures 3, 9 and 14 for Examples 1–3, respectively. From these figures it can be seen that there is good agreement between the exact solutions and the numerical solutions obtained with $\alpha = 0$. Regularization with $\alpha \neq 0$ does not seem to improve further the accuracy of the numerical solutions $f_{1\mathrm{h}}(x_1, x_2)$. The above conclusion is more clearly illustrated by taking a slice through the plane $x_2 = 0.5$ and comparing in the left-hand sides of Figures 5, 11 and 16 the numerical solutions $f_{1\mathrm{h}}(x_1, 0.5)$ with the exact solutions $f_1(x_1, 0.5)$ for Examples 1–3, respectively. Finally, the left-hand sides of Figures 6, 12 and 17 show the numerical solutions $f_{2\tau}$ in comparison with the exact solutions $f_2(t)$ for Examples 1–3, respectively. From these figures it can be seen that the numerical solution $f_{2\tau}(t)$ obtained with no regularization, i.e. $\alpha = 0$, is slightly oscillatory, but this instability can be alleviated by the inclusion of some small regularization with $\alpha \neq 0$. Finally, we wish to mention that in the case of input data without noise the choice of $\alpha \neq 0$ is irrelevant since most of the results are stable and accurate as obtained using $\alpha = 0$, and in any case, the stability of the numerical solutions should be tested for noisy data, as described in the next subsection.

5.2 Input Data With Noise

We next consider the case of noise data, i.e. the input data (2.6) and (2.18) is contaminated by some random noise $\delta_1 = \delta_2 \in \{5 \times 10^{-4}, 10^{-3}, 10^{-2}\}$ which is introduced in order to test the stability of the numerical solution, as well as to model the errors which are inherently present in any practical measurement. In this case, we can take $\alpha = 0$, but then we will stop the CGM according to the stopping rule (5.1).

The stopping iteration numbers n^*, the errors $\|f_1 - f_{1n^*}\|_{L^2(\Omega)}$ and $\|f_2 - f_{n^*}\|_{L^2(0,T)}$ and the values of the objective function $J_0(f_{n^*})$ are given in Tables 1–3 for Examples 1–3, respectively. The decreasing monotonic behaviour of $J_0(f_n)$, as a function of the number of iterations n, is also illustrated in the right-hand sides of Figures 1 and 7 for Examples 1 and 2, respectively. From these tables and figures it can be seen, as expected, that the stopping iteration number $n^*(\delta)$ is a decreasing function of the amount of noise δ. Also, the numerical results become more accurate and the objective function J_0 decreases as the amount of noise δ decreases. Finally, we observe that the values of n^* are relatively small which show that the CGM is a much faster regularizing algorithm compared to other much slower iterative algorithms such as the Landweber method for example.

For $\delta_1 = \delta_2 \in \{5 \times 10^{-4}, 10^{-3}\}$ noise, the numerical solutions $f_{1\mathrm{h}}(x_1, x_2)$ are shown in comparison with the exact solutions $f(x_1, x_2)$ in Figures 4, 10 and 15 for Examples 1–3, respectively. From these figures it can be seen that the numerical solutions are stable and reasonably accurate. The numerical results for a larger amount of noise such as $\delta_1 = \delta_2 = 10^{-2}$ are not illustrated in these figures because the numerical solutions obtained in this case were oversmoothed by the discrepancy principle (5.1). All these conclusions are further clearly illustrated in the right-hand side of Figures 5, 11 and 16 for Examples 1–3, respectively.

Finally, the results presented in the right-hand sides of Figures 6, 12 and 17 for Examples 1–3, respectively, show that the numerical solutions $f_{2\tau}(t)$ are stable and reasonably accurate predictions of the exact solutions $f_2(t)$ for all the amounts of noise considered. We also observe that there is no significant dependence (on t) of the numerical results as t increases, vis-a-vis of the local uniqueness solvability result of Theorem 2.1

$\delta_1 = \delta_2$	n^*	$\|f_1 - f_{1n^*}\|_{L^2(\Omega)}$	$\|f_2 - f_{2n^*}\|_{L^2(0,T)}$	$J_0(f_{n*})$
5×10^{-4}	123	0.1586	0.0829	2.98E-7
10^{-3}	60	0.1760	0.0848	1.18E-6
10^{-2}	13	0.2966	0.1133	1.06E-4

Table 3: The results for Example 3 with noise.

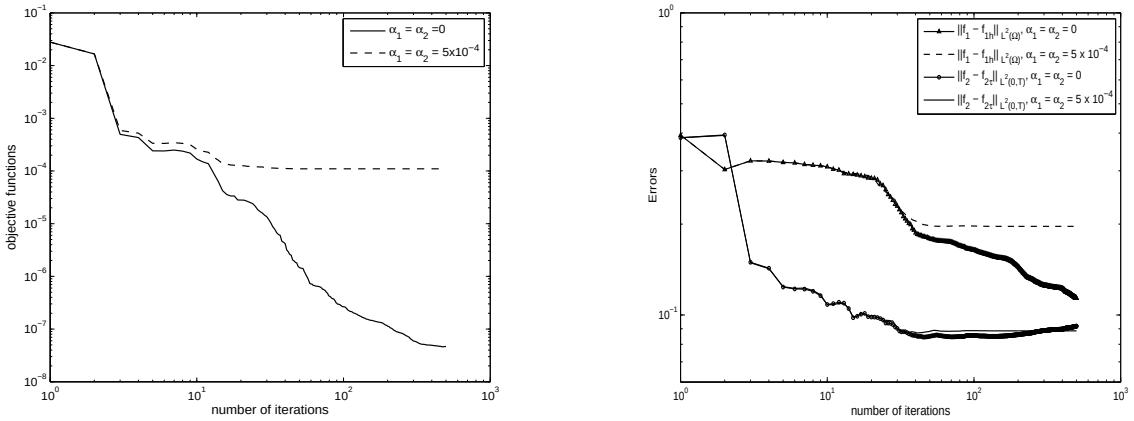

Figure 13: The objective functions (left) and the L^2-errors (right) for Example 3 without noise.

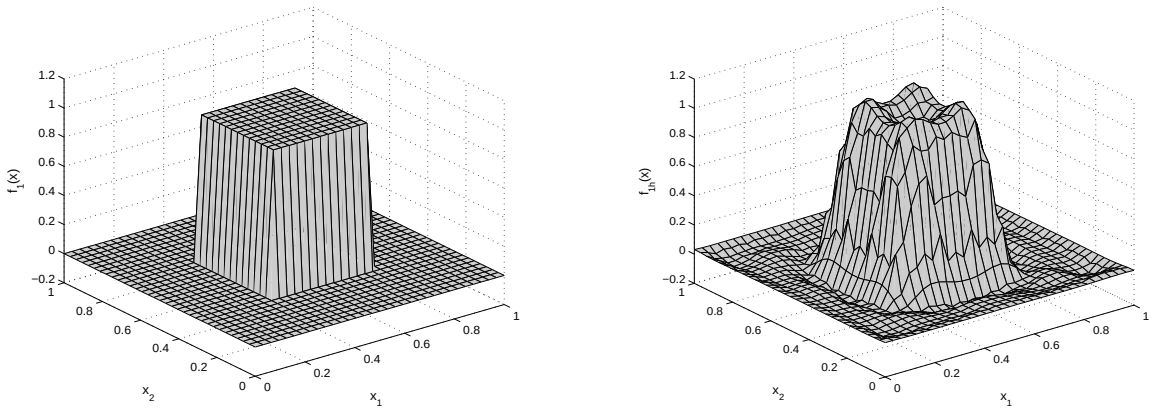

Figure 14: The exact solution $f_1(x)$ (left) and the approximate solution $f_{1\mathrm{h}}(x)$ without noise obtained with $\alpha_1 = \alpha_2 = 0$ (right) for Example 3.

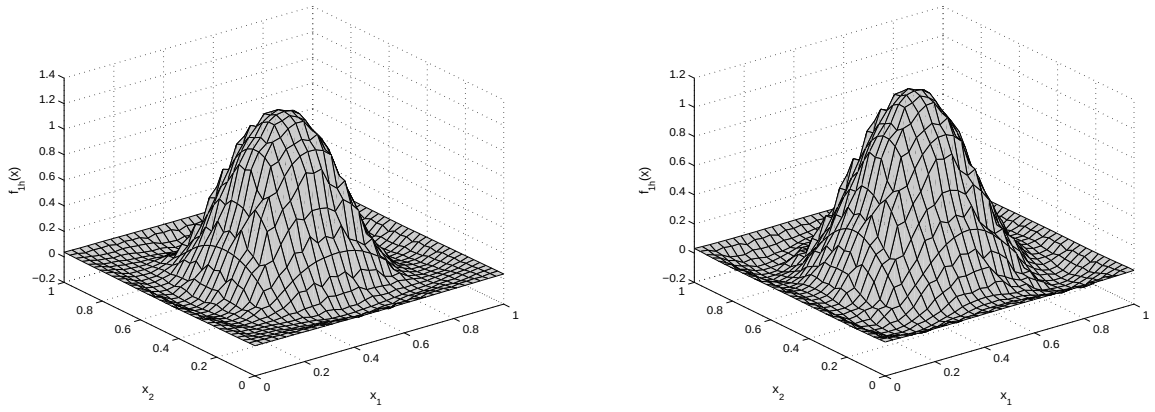

Figure 15: The approximate solutions $f_{1\mathrm{h}}(x)$ with noise $\delta_1 = \delta_2 = 5\times10^{-4}$ (left) and $\delta_1 = \delta_2 = 10^{-3}$ (right) for Example 3.

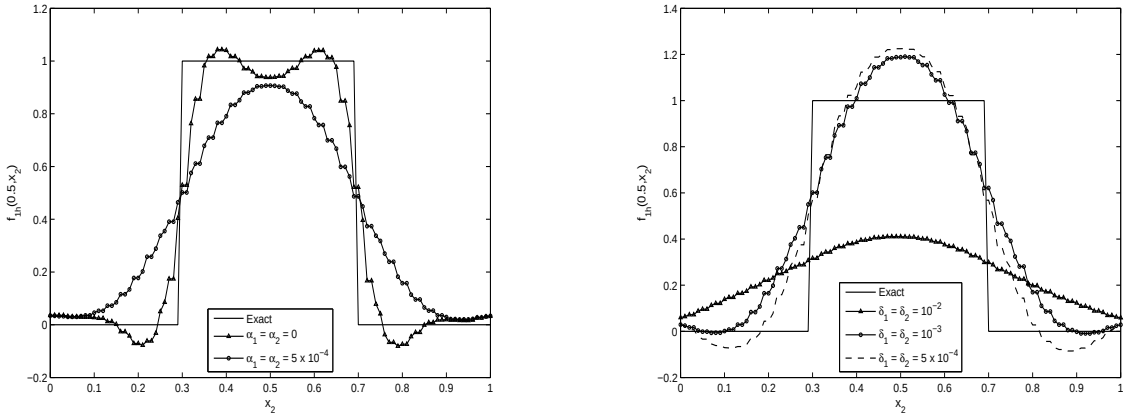

Figure 16: The approximate solutions $f_{1\mathrm{h}}(x_1, 0.5)$ without noise (left) and with noise (right) for Example 3.

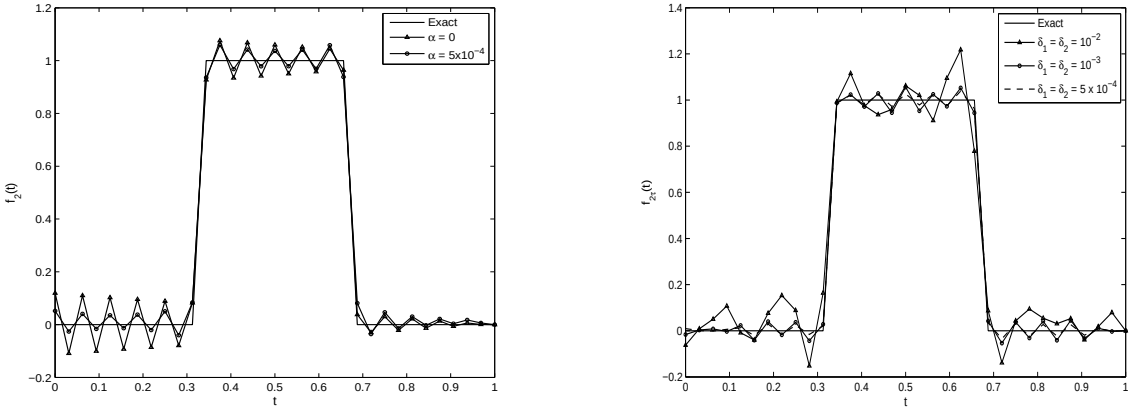

Figure 17: The approximate solutions $f_{2\tau}(t)$ without noise (left) and with noise (right) for Example 3.

6 Conclusions

A novel inverse heat source problem with integral observations has been investigated. The local existence and uniqueness of a classical solution have been established and furthermore, a variational formulation has been proposed. The numerical method for obtaining a stable solution was based on the FEM combined with the CGM. The numerical results demonstrate that accurate and stable numerical solutions can be obtained. There seems to be a balance between predicting simultaneously the space and time-dependent components of the additive source. Moreover, as expected, the reconstruction of the multi-dimensional space component is more difficult than the single-dimension time component of the source. Future work may consist into developing the analysis of this study for recovering a heat source which separates as the product, rather than sum, of two unknown functions; one which depends on space and one which depends on time. However, in this situation the inverse problem becomes nonlinear and the details appear more complicated. All the above programme builds upon ultimately attacking the challenging inverse problem of retrieving a heat source which depends on both space and time variables in a general way.

Acknowledgements

This research was supported by a Marie Curie International Incoming Fellowship within the 7th European Community Framework Programme, the London Mathematical Society, and by Vietnam National Foundation for Science and Technology Development (NAFOSTED) under grant number 101.02-2011.50.

References

[1] El Badia A. and Ha-Duong T., On an inverse source problem for the heat equation. Application to a pollution detection problem. *J. Inverse Ill-Posed Probl.* 10(2002), 585–599.

[2] Evans L.C., *Partial Differential Equations*, Amer. Math. Soc., Providence, Rhode Island, 2002.

[3] Farcas A. and Lesnic D., The boundary-element method for the determination of a heat source dependent on one variable. *J. Engrg. Math.* 54(2006), 375–388.

[4] Gol'dman N.L., Properties of solutions of parabolic equations with an unknown right-hand side and of their conjugate problems. *Dokl. Math.* 77(2008), 350–355.

[5] Hanke M., *Conjugate Gradient Type Methods for Ill-Posed Problems*. Longman Scientific & Technical, Harlow, 1995.

[6] Dinh Nho Hào, Phan Xuan Thanh, Lesnic D., and Johansson B.T., A boundary element method for a multi-dimensional inverse heat conduction problem. *Int. J. Comput. Math.* 89(2012), 1540–1554.

[7] Hasanov A. and Pektas B., Identification of an unknown time-dependent heat source term from overspecified Dirichlet boundary data by conjugate gradient method. *Comput. Math. Appl.* 65(2013), 42–57.

[8] Hasanov A. and Slodicka M., An analysis of inverse source problems with final time measured output data for the heat conduction equation: a semigroup approach. *Appl. Math. Lett.* 26(2013), 207–214.

[9] Hinze M. A variational discretization concept in control constrained optimization: The linear-quadratic case, *Computat. Optimiz. Appl.*, 30(2005), 45–61.

[10] Isakov V., *Inverse Problems for Partial Differential Equations.* Second edition. Springer, New York, 2006.

[11] Ivanchov M.I., Inverse problem for a multidimensional heat equation with an unknown source function. *Mat. Stud.* 16(2001), 93–98.

[12] Johansson B.T. and Lesnic D., A variational method for identifying a spacewise-dependent heat source. *IMA J. Appl. Math.* 72(2007), 748–760.

[13] Johnson C., *Numerical Solution of Partial Differential Equations by the Finite Element Method.* Cambridge University Press, Cambridge, 1987.

[14] Ladyzhenskaya O.A., Solonnikov V.A., and Ural'ceva N.N., *Linear and Quasilinear Equations of Parabolic Type*, AMS, Providence, 1967.

[15] Nemirovskii A.S., The regularizing properties of the adjoint gradient method in ill-posed problems. *Zh. vychisl. Mat. mat. Fiz.* 26(1986), 332–347. Engl. Transl. in *U.S.S.R. Comput. Maths. Math. Phys.*, 26(2)(1986), 7–16.

[16] Plato R., The conjugate gradient method for linear ill-posed problems with operator perturbations. *Numer. Algorithms* 20(1999), 1–22.

[17] Prilepko A.I. and Solov'ev V.V., Solvability theorems and the Rothe method in inverse problems for an equation of parabolic type. I. *Differential Equations* 23(1987), 1230–1237.

[18] Prilepko A.I. and Tkachenko D.S., Inverse problem for a parabolic equation with integral overdetermination. *J. Inverse Ill-Posed Probl.* 11(2003), 191–218.

[19] Rundell W., Determination of an unknown nonhomogeneous term in a linear partial differential equation from overspecified boundary data. *Applicable Anal.* 10(1980), 231–242.

[20] Savateev E.G., On problems of determining the source function in a parabolic equation. *J. Inverse Ill-Posed Probl.* 3(1995), 83–102.

[21] Tröltzsch F., *Optimale Steuerung partieller Differentialgleichungen*, Vieweg + Teubner, Wiesbaden, 2005.